PNAS
www.pnas.org

Heme ameliorates dextran sodium sulfate-induced colitis through providing intestinal macrophages with non-inflammatory profiles

Hisako Kayama[1,2,3#], Masako Kohyama[4, 5#], Daisuke Okuzaki[6], Daisuke Motooka[6], Soumik Barman[1,2,3], Ryu Okumura[1,2,3], Masato Muneta[1], Katsuaki Hoshino[11], Izumi Sasaki[8], Wataru Ise[12], Hiroshi Matsuno[10], Junichi Nishimura[10], Tomohiro Kurosaki[12], Shota Nakamura[6], Hisashi Arase[4, 5], Tsuneyasu Kaisho[7, 8, 9*], and Kiyoshi Takeda[1,2,3]

Corresponding author: Kiyoshi Takeda

Laboratory of Immune Regulation, Department of Microbiology and Immunology, Graduate School of Medicine, Osaka University,

2-2 Yamadaoka, Suita, Osaka 565-0871, Japan

Tel: +81-6-6879-3980, Fax: +81-6-6879-3989

E-mail: ktakeda@ongene.med.osaka-u.ac.jp

and Tsuneyasu Kaisho

Department of Immunology, Institute of Advanced Medicine, Wakayama Medical University,

811-1 Kimiidera, Wakayama, Wakayama 641-8509

Tel: +81-73-441-0606, Fax: +81-73-445-5585

E-mail: tkaisho@wakayama-med.ac.jp

www.pnas.org/cgi/doi/10.1073/pnas.1808426115

and Hisako Kayama

Laboratory of Immune Regulation, Department of Microbiology and Immunology,

Graduate School of Medicine, Osaka University,

2-2 Yamadaoka, Suita, Osaka 565-0871, Japan

Tel: +81-6-6879-3982, Fax: +81-6-6879-3989

E-mail: kayama@ongene.med.osaka-u.ac.jp

This PDF file includes:

Supplementary text
Figs. S1 to S6
Tables S1 to S2

SI Materials and Methods

Generation of floxed-*Spic* mice

To generate the *Spic*-targeted mice, a targeting vector was designed to delete exon 6 encoding the Ets domain of Spi-C. To construct the targeting vector, C57BL/6N mouse genomic DNA fragments were amplified by PCR using KOD -plus- DNA polymerase (Toyobo, Osaka, Japan). A 6.8 kbp long arm containing exons 2-6, which has insertion of a loxP site in the intron between exon 5 and 6, was connected to a phosphoglycerate kinase promoter-driven neomycin resistance cassette (neo) flanked by two FRT sites and a loxP site. Then, a 2.0 kbp short arm was ligated to downstream of the neo cassette. A herpes simplex virus thymidine kinase gene (HSV-TK) was attached at the upstream end of the long arm. The targeting vector was linearized with *Sal*I and electroporated into a C57BL/6N-derived embryonic stem cell line, JM8A3.N1. The clones with resistance to G418 and gancyclovir were screened for homologous recombination by PCR and confirmed by Southern blot analysis with the probe shown in Fig. S2A. ES clone no. 58 shown in Fig. S2A was used to generate chimeric and the *Spic*-targeted mice. To delete the neo cassette flanked by two FRT sites, the *Spic*-targeted mice were intercrossed with C57BL/6-Tg(CAG-FLPe) 36Ito/ItoRbrc mice (RBRC01834) (RIKEN BioResurce Center, Japan)(1).

Generation of *Lyz2-cre; Spic*$^{flox/flox}$ mice

Lyz2-cre transgenic mice (The Jackson Laboratory) were bred with *Spic*$^{flox/+}$ mice to generate mice carrying *Lyz2-cre* and heterozygous *Spic* flox (*Lyz2-cre; Spic*$^{flox/+}$) genes. These mice were mated with *Spic*$^{flox/flox}$ mice. Offspring carrying *Lyz2-cre* and floxed *Spic* genes (*Lyz2-cre; Spic*$^{flox/flox}$) and floxed *Spic* genes (*Spic*$^{flox/flox}$) were used for further experiments. The floxed *Spic* mice were backcrossed to C57BL/6J mice for at least six generations.

Reagents

The Ca^{2+} ionophore A23187, phorbol myristate acetate (PMA), lipopolysaccharide (O55: B5), and an anti-β-actin antibody (clone AC-74) were purchased from Sigma-Aldrich (St. Louis, MO, USA). Dextran sulfate sodium salt (DSS) was purchased from MP Biomedicals (Kaysersberg, France). Anti-GFP (clone B-2), anti-HA (clone F-7), and anti-p65 (C-20) antibodies were purchased from Santa Cruz Biotechnology (Dallas, TX, USA). An anti-His antibody (clone 291-3) was purchased from MBL Co., Ltd. (Nagoya, Aichi, Japan). An anti-IRF5 antibody (ab21689) and iron stain (ab150674) were purchased from Abcam (Cambridge, UK). Hemoglobin Colorimetric Assay Kit was purchased from Cayman Chemical Company (Ann Arbor, MI, USA). Iron Assay Kit was purchased from Metallogenics Co., Ltd. (Chiba, Chiba, Japan). The AIN93G and iron-reduced diets were manufactured by Oriental Yeast (Tokyo, Japan).

Preparation of Mϕs

To generate BMDMϕs, bone marrow cells were prepared from mouse femurs and tibias, passed through a nylon mesh, and cultured in RPMI 1640 culture medium (10% fetal bovine serum, 100 μg/ml streptomycin, 100 U/ml penicillin, and 100 μM 2-mercaptoethanol) with 50 ng/ml M-CSF (R&D Systems, Minneapolis, MN, USA). After 14 days, the adherent cells were used as M-CSF-induced BMDMϕs. To induce PB-MOMϕs, $CD11b^{+}$ Ly-$6C^{high}$ monocytes from blood were cultured in RPMI 1640 culture medium containing 50 ng/ml M-CSF for 14 days. BMDMϕs and PB-MOMϕs were pretreated with 40 μM hemin for 18 h and stimulated with LPS for 24 h. The culture supernatants were used for the analysis of proinflammatory cytokine production.

Flow cytometry

The following antibodies were purchased from BD Biosciences: anti-mouse CD16/32 (clone 2.4.G2), PE-Cy7-conjugated anti-mouse-Ly-6C (clone AL-21), and APC-

conjugated anti-mouse-CD11c (clone HL3). PE-conjugated anti-mouse CX_3CR1 (clone SA011F11), APC-conjugated anti-mouse F4/80 (clone BM8), Pacific blue-conjugated anti-mouse CD11b (clone M1/70), Percp-Cy5.5-conjugated anti-mouse CD4 (clone CK1.5), APC-conjugated anti-mouse IL-17A (clone TC11-18H10.1), FITC-conjugated anti-mouse IFN-γ (clone XMG1.2), PE-conjugated anti-mouse IL-10 (clone JES5-16E3), and FITC- or PE/Cy7-conjugated anti-mouse CD45 (clone 30-F11) antibodies were purchased from BioLegend. APC-conjugated anti-mouse Foxp3 antibody (clone 3G3) was purchased from TONBO Biosciences (Tucson, AZ, USA). For dead cell exclusion, 7-AAD (BD Biosciences) and Fixable Viability Stain 510 (BD Biosciences) were used. Flow cytometric analysis was performed with a FACSCanto II flow cytometer (BD Biosciences) with FlowJo software (Tree Star, Ashland, OR, USA). Murine splenic $CD11b^-$ $F4/80^+$ RPMϕs, murine blood $CD11b^+$ $Ly\text{-}6C^{high}$ monocytes, and murine large intestinal innate myeloid cell subsets were isolated with a FACSAria flow cytometer (BD Biosciences). The instrumental compensation was set in each experiment using two-color, three-color, four-color, and six-color stained samples.

Quantitative RT-PCR

Total RNA was isolated using the RNeasy Mini Kit (Qiagen, Manchester, UK), and the RNA was reverse transcribed with Moloney Murine Leukemia Virus Reverse Transcriptase (M-MLV) (Promega, Madison, WI, USA) and random primers (Toyobo, Tokyo, Japan) after treatment with RQ1 DNase I (Promega). Quantitative RT-PCR was performed on a Step One Plus™ Real-Time PCR System (Applied Biosystems) using GoTaq qPCR Master Mix (Promega). All values were normalized to the expression of *Gapdh*, encoding glyceraldhyde-3-phosphate dehydrogenase, and the fold difference in expression relative to that of *Gapdh* is shown. The amplification conditions were 50 °C (2 min), 95 °C (10 min), and 40 cycles of 95 °C (15 s) and 60 °C (60 s). The following

primer sets were used: *Gapdh*, 5′-CCTCGTCCCGTAGACAAAATG-3′ and 5′-TCTCCACTTTGCCACTGCAA-3′;
Il6, 5′-CTGCAAGAGACTTCCATCCAGTT-3′ and 5′-AAGTAGGGAAGGCCGTGGTT-3′; *Tnf* , 5′- TCCAGGCGGTGCCTATGT-3′ and 5′-CACCCCGAAGTTCAGTAGACAGA-3′; *Il1a*, 5′-CAGTCCATAACCCATGATCT-3′ and 5′-ATCATTCATGACAAACTTCT-3′; *Spic*, 5′-TGCCTCTGGCTTTGTCAACC-3′ and 5′-TCTTCCAGCAAAAGGGAGGA-3′; *Hmox1*, 5′-CTGCTAGCCTGGTGCAAGATACT-3′ and 5′-GTCTGGGATGAGCTAGTGCTGAT-3′; *Slc40a1*, 5′-CCCTGCTCTGGCTGTAAAAG-3′ and 5′-TCTTTCTCACCCATTAGATG-3′; *Blvrd*, 5′-TCGAGGGCCCTCGTCCATCC-3′ and 5′-GGATGCATAAGATTCTGCAA-3′; and *Lyz2*, 5′-CCTGTGGGATCAATTGCAGT-3′ and 5′-CCATGCCACCCATGCTCGAA-3′.

Isolation of murine intestinal lamina propria cells

Murine innate myeloid cells and $CD4^+$ lymphocytes were isolated from large intestinal lamina propria using a previously described protocol (2).

Induction of DSS-induced colitis

Eight-to twelve-week-old *Spic* mutant mice and their littermate control mice were administered with 1.5% DSS (36–50 kDa) in the drinking water for 7 days to induce acute colitis. Mice were analyzed for changes in weight and large intestinal histology. Large intestines collected from mice after the initiation of 1.5% DSS administration were fixed in 4% paraformaldehyde. Paraffin-embedded sections mounted on glass slides were used for Hematoxylin-Eosin (H&E) staining and images of H&E staining were taken using Biozero (KEYENCE, Osaka, Japan). Each section of the large intestine was evaluated using inflammation scores, as described previously(3). In mice administered with DSS, the severity of colitis were evaluated as previously reported(4). To analyze the

production of cytokines by whole colons, the colons were opened longitudinally and washed in PBS supplemented with penicillin and streptomycin to remove feces. The colons were treated with HBSS containing 5 mM EDTA for 20 min at 37°C on a shaker and rubbed against a paper towel to remove the epithelial cells. The tissues were cut into small pieces and cultured in 24-well flat-bottom culture plates in serum-free RPMI 1640 medium supplemented with penicillin and streptomycin. After 24 h, the culture supernatants were collected and used for the analysis of cytokine production.

Determination of microbiota by deep sequencing

Extraction of bacteria DNA from feces was performed according to the protocol described in previous report(5). Libraries were prepared according to "Illumina 16S Metagenomic Sequencing Library Preparation Guide" with a primer set (27Fmod: 5′-AGRGTTTGATCMTGGCTCAG-3′ and 338R: 5′-TGCTGCCTCCCGTAGGAGT-3′) targeting the V1–V2 region of the 16S rRNA gene. 251 bp paired end sequencing of the amplicon was performed on a MiSeq (Illumina) using MiSeq v2 500 cycle kit. Raw sequences were demultiplexed and quality-trimmed with the FASTX-Toolkit (hannonlab.cshl.edu/fastx_toolkit/index.html) and BBtrim (bbmap.sourceforge.net). 30,000 reads per sample were randomly selected using seqtk (https://github.com/lh3/seqtk) for further analysis. The processed sequences were clustered into OTUs defined at a 97% similarity cutoff using UCLUST version 1.2.22q. Representative sequences for each OTU were then classified taxonomically by using RDP Classifier version 2.2, with the Greengenes 13_8 database. The bioinformatics pipeline QIIME, version 1.9.1, was used as the informatics environment for all relevant processing of raw sequencing data and calculation of bacterial relative abundances.

Intracellular cytokine staining

Spleen, MLN, and large intestinal $CD4^+$ T cell intracellular IFN-γ, IL-10, and IL-17A expression was analyzed with a Cytofix/Cytoperm Plus Kit with GolgiStop (BD Biosciences), according to the manufacturer's instructions. In brief, $CD4^+$ T cells isolated from the large intestinal lamina propria of mice were incubated with 50 ng/ml PMA, 5 μM calcium ionophore A23187, and GolgiStop in complete RPMI 1640 at 37 °C for 4 h. Surface staining was performed with anti-CD4 antibody for 20 min at 4 °C and intracellular cytokine staining was performed with the indicated antibodies for 20 min.

Generation of RAW264.7 cells stably expressing Spi-C

RAW264.7 cells were co-transfected with linearized empty pcDNA3.1 (+) vector (Invitrogen) and linearized pCAGGS vector (Addgene) inserted into the sequence for Spi-C-His using nucleofection (Nucleofector Kit for Mouse Macrophages; Lonza). These cells were cultured in G418-containing complete RPMI 1640. Clones resistant to G418 were selected and screened for the expression of Spi-C-His by western blot using anti-His antibody and quantitative RT-PCR.

DNA microarray analysis

$CD11c^{high}$ $CD11b^-$ DCs, $CD11c^-$ $CD11b^+$ cells, $CX3CR1^{high}$ Mϕs, and $CD11c^+$ $CD11b^+$ $CX3CR1^-$ cells were collected from the lareg intestinal lamina propria of C57BL/6J mice. Total RNA was extracted with an RNeasy kit (Qiagen). RNA quality was assessed using an Agilent Bioanalyzer 2100 and only RNA with minimal degradation and distinct 18S and 28S rRNA bands were used for DNA microarray analysis. Fragmented and biotin-labeled cDNA was synthesized from 100 ng purified mRNA with the GeneChip 3'IVT Express Kit Assay (Affymetrix). The cDNA was hybridized to Mouse Genome 430A 2.0 Array (Affymetrix). Hybridized chips were stained, washed, and scanned with GeneChip Scanner 3000 (Affymetrix) according to manufacturer instructions. The CEL files were performed a MAS5.0 normalization using Genespring software version 14.8 (Agilent

Technologies). The differentially expressed probes with 2-fold changes up>2.0 (CX3CR1^{high} Mϕs cells vs. others) were calculated using Subio Basic Plug-in (Subio) followed by extracting lists of probe set IDs that were flagged Present in all samples. A total of 239 probe sets were used for further analysis. These results have been deposited in the National Center Biotechnology Information (NCBI) Gene Expression Omnibus database (GSE100804).

RNA-seq analysis

Control and *Spic*$^{-/-}$ BMDMϕs pretreated with 40 μM hemin for 18 h were stimulated with (designated 'CNT_4' and 'cKO_4', respectively) or without (designated 'CNT_0' and 'cKO_0', respectively) 100 ng/ml LPS for 4 h. Total RNAs were extracted from these cells using a RNeasy Mini Kit (Qiagen). Library preparation was performed using a TruSeq stranded mRNA sample prep kit (Illumina, San Diego, CA) according to the manufacturer's instructions. Sequencing was performed on an Illumina HiSeq 2500 platform in the 75-base single-end mode. Illumina Casava1.8.2 software was used for base calling. Sequenced reads were mapped to the mouse reference genome sequences (mm10) using TopHat v2.0.13 in combination with Bowtie2 ver. 2.2.3 and SAMtools ver. 0.1.19. The fragments per kilobase of exon per million mapped fragments (FPKMs) were calculated using Cuffnorm version 2.2.1. Among the calculated genes with a normalized FPKM value ≥ 0.1 in CNT_4, 85 genes were up-regulated ≥ 3.0-fold from cKO_0 to cKO_4 and ≥ 1.74-fold from CNT_4 to cKO_4 (Table S2). These results have been deposited in the National Center Biotechnology Information (NCBI) Gene Expression Omnibus database (GSE100805).

Cytokine analysis

The concentrations of IL-6, TNF-α, IL-1α, IL-10, IL-17A, and IFN-γ in culture

supernatants or blood serum were measured with a Cytometric Bead Array (CBA) kit (BD Biosciences).

Primer sets for ChIP assay

The primer sequences were: *Il6*; 5′-ACCCTCACCCTCCAACAA-3′ and 5′-GTCCTATATTTATTGGGGGT-3′, *Tnf*; 5′-CACCAAGGAAGTTTTCCGAG-3′ and 5′-CTTGCTGTCCTCGCTGAGGG-3′, and *Il1a*; 5′-TCCTCAAGCAGGTAGGAGTG-3′ and 5′-GGCCGGTATCAGGCAGAATG-3′.

Figure S1

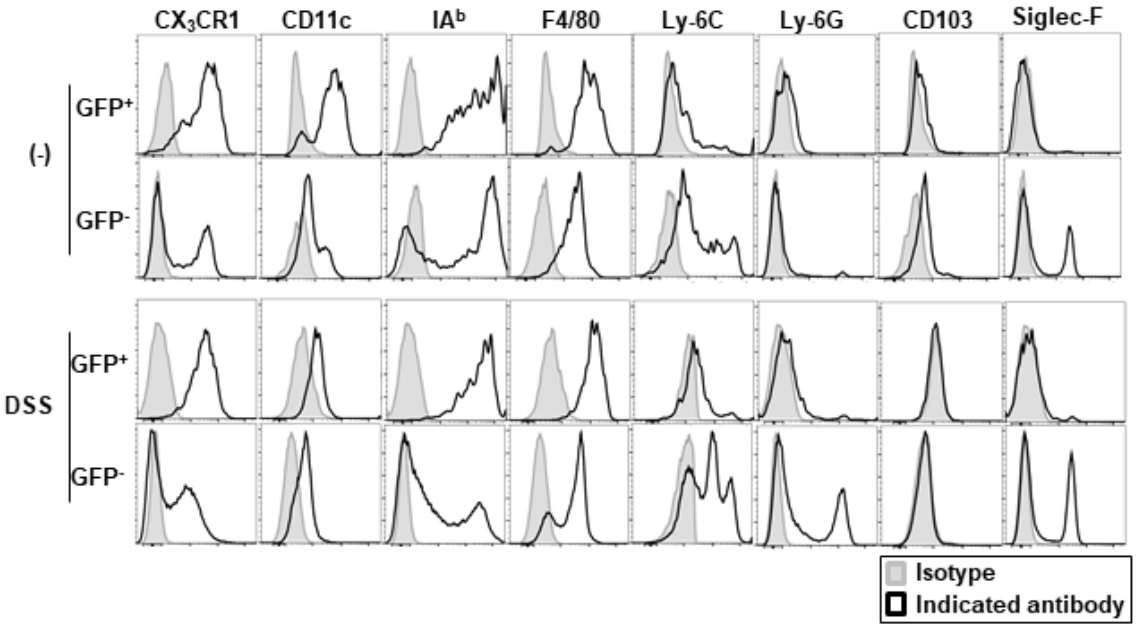

Fig. S1: Expression of Spi-C in murine innate myeloid cells from the colon.
Large intestinal lamina propria cells were isolated from *Spic*$^{\text{IRES-GFP/GFP}}$ mice administered with or without 1.5% DSS for 5days. Surface expression of CX_3CR1, CD11c, IA^b, F4/80, Ly-6C, Ly-6G, CD103, and Siglec-F on Spi-C-positive $CD11b^+$ (GFP^+) and Spi-C-negative $CD11b^+$ (GFP^-) cells among $CD45^+$ living cells. Filled histograms, isotype control. All data are representative of two independent experiments.

Figure S2

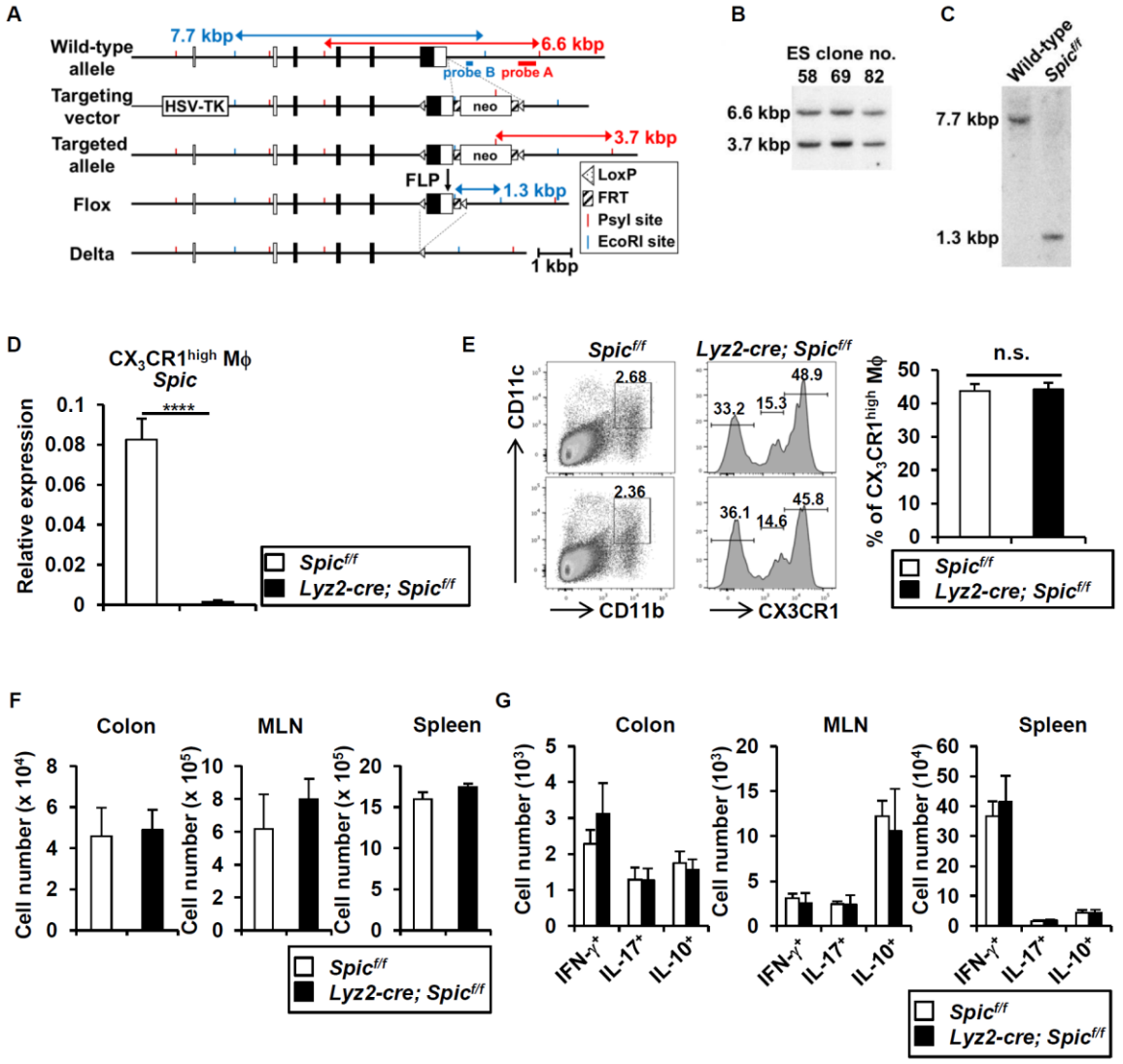

Fig. S2: Lack of *Spic* expression in intestinal Cx_3CR1^{high} Mϕ of in *Lyz2-cre; Spic$^{flox/flox}$* mice. **(A)** Map of the Spi-C wild-type genome, targeting vector, and predicted targeted gene. Open boxes, noncoding exons; closed boxes, coding exons. **(B)** Southern blot analysis of ES clones. Genomic DNA from ES cells was digested with PsyI, separated electrophoretically, and then hybridized with the probe A (indicated by red) as shown in A. Approximate sizes of the wild-type and targeted bands are 6.6 and 3.7 kbp, respectively. **(C)** Southern blot analysis of wild-type or homozygous floxed mice. Genomic DNA from mice was digested with EcoRI, electrophoresed, and hybridized with the probe B (indicated by blue) as shown in A. Approximate sizes of the wild-type and floxed bands are 7.7 and 1.3 kbp, respectively. **(D)** Expression of *Spic* in large intestinal CX_3CR1^{high} Mϕs from control and *Spic* mutant mice (means values ± SEM from four independent experiments). $^{****}p < 0.001$. **(E)** Flow cytometric blots of the cells isolated from the colons of control and *Spic* mutant mice (left). Histograms show the expression of CX_3CR1 on large intestinal $CD11b^+$ $CD11c^+$ cells (middle). Frequencies of CX_3CR1^{high} Mϕs in large intestinal $CD11b^+$ $CD11c^+$ cells (right). n.s., not significant. Mean values ± SEM from four independent experiments. **(F, G)** The numbers of $Foxp3^+$ $CD4^+$ T cells (F), IFN-γ–, IL-17–, and IL-10–producing $CD4^+$ T cells (G) in the indicated tissues from control and *Spic* mutant mice in the steady state (mean values ± SEM). All data are generated from 2 independent experiments. n = 6 in each group.

Figure S3

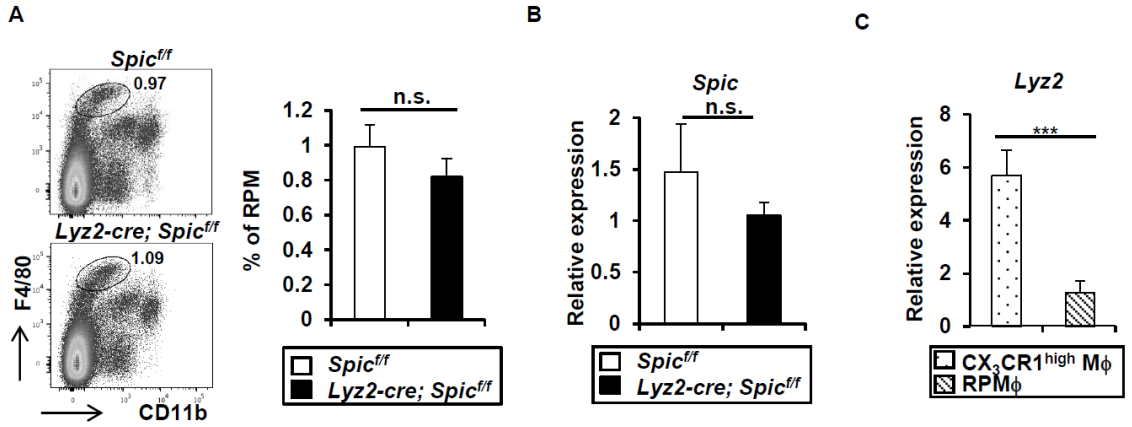

Fig. S3: RPMϕs are present normally in the spleen of *Lyz2-cre; Spic*$^{flox/flox}$ mice.
(A) Flow cytometry analysis of cells from the spleens of control (n = 6) and *Spic* mutant (n = 4) mice (left). Frequencies of CD11b^{-} F4/80^{high} RPMϕs in the spleens (right). All graphs show the means ± SD. n.s., not significant. All data are of four independent experiments. **(B)** Expression of *Spic* in RPMϕs from control and *Spic* mutant mice (means values ± SEM from four independent experiments). **(C)** Expression of *Lyz2* in RPMϕs and intestinal CX_3CR1^{high} Mϕs. ***$p < 0.005$. Graphs show the means ± SEM from four independent experiments.

Figure S4

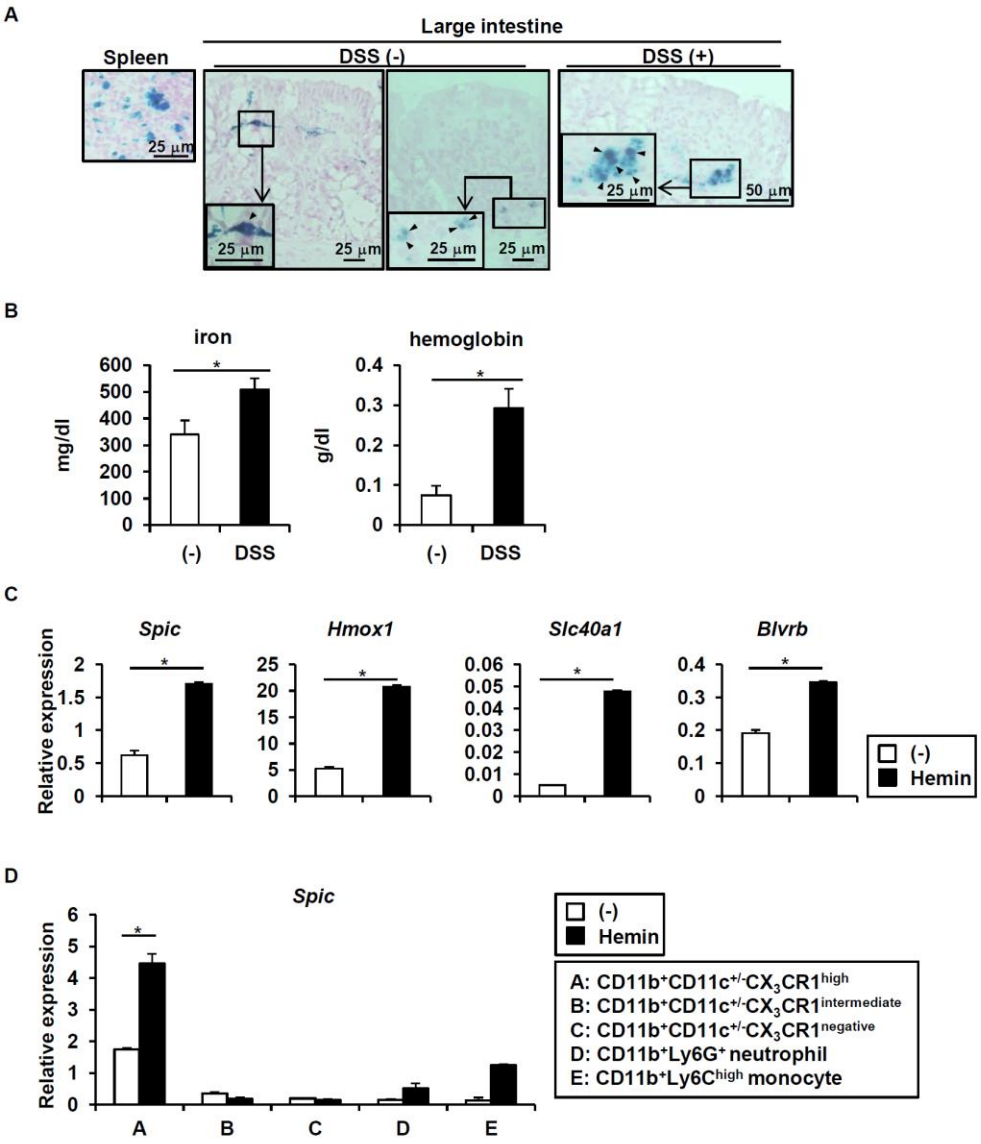

Fig. S4: The presence of heme in the colon and heme-mediated induction of *Spic* in innate myeloid cells. (A) Ferric iron of the spleen and colon from C57BL/6J mice administered with or without 1.5% DSS for 5 days were detected with the prussian blue reaction. Arrowheads indicate ferric iron. Insert at the lower left-hand corner of each panel is an engaged image of the boxed area. Data are representative of three independent experiments. **(B)** Concentration of iron and hemoglobin in large intestinal luminal contents from mice administered with (n = 6) or without DSS (n = 11) (means ± SEM). Data are of three independent experiments. $^{*}p < 0.05$. **(C, D)** C57BL/6J mice were intraperitoneally injected with 1 mg hemin. After 2 days, $CD11b^{+}$ $CD11c^{+}$ cells (C) and the indicated cell subsets (D) were isolated from the colon and analyzed for the expression of the indicated genes. Graphs show the mean ± SEM of three independent experiments. $^{*}p < 0.05$.

Figure S5

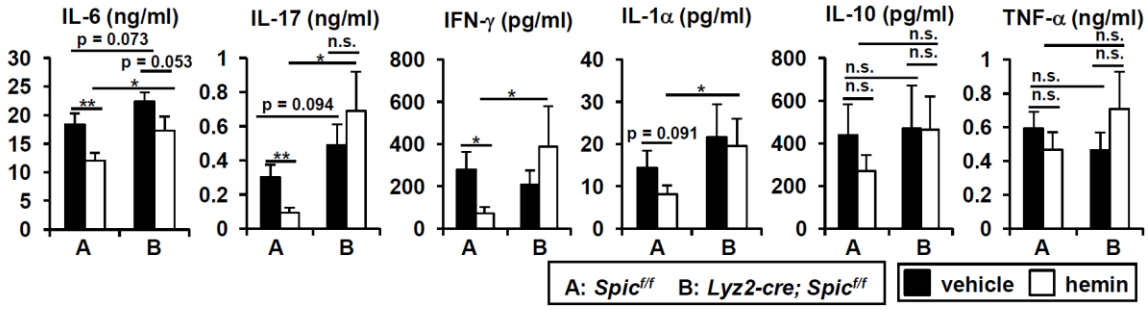

Fig. S5: Effect of hemin on cytokines production in the colon of *Spic*$^{flox/flox}$ and *Lyz2-cre; Spic*$^{flox/flox}$ mice administered with DSS. Cytokine production from colon explants after DSS administration. $^{*}p < 0.05$, $^{**}p < 0.01$. All graphs show the mean ± SEM from two separate experiments. n.s., not significant.

Figure S6

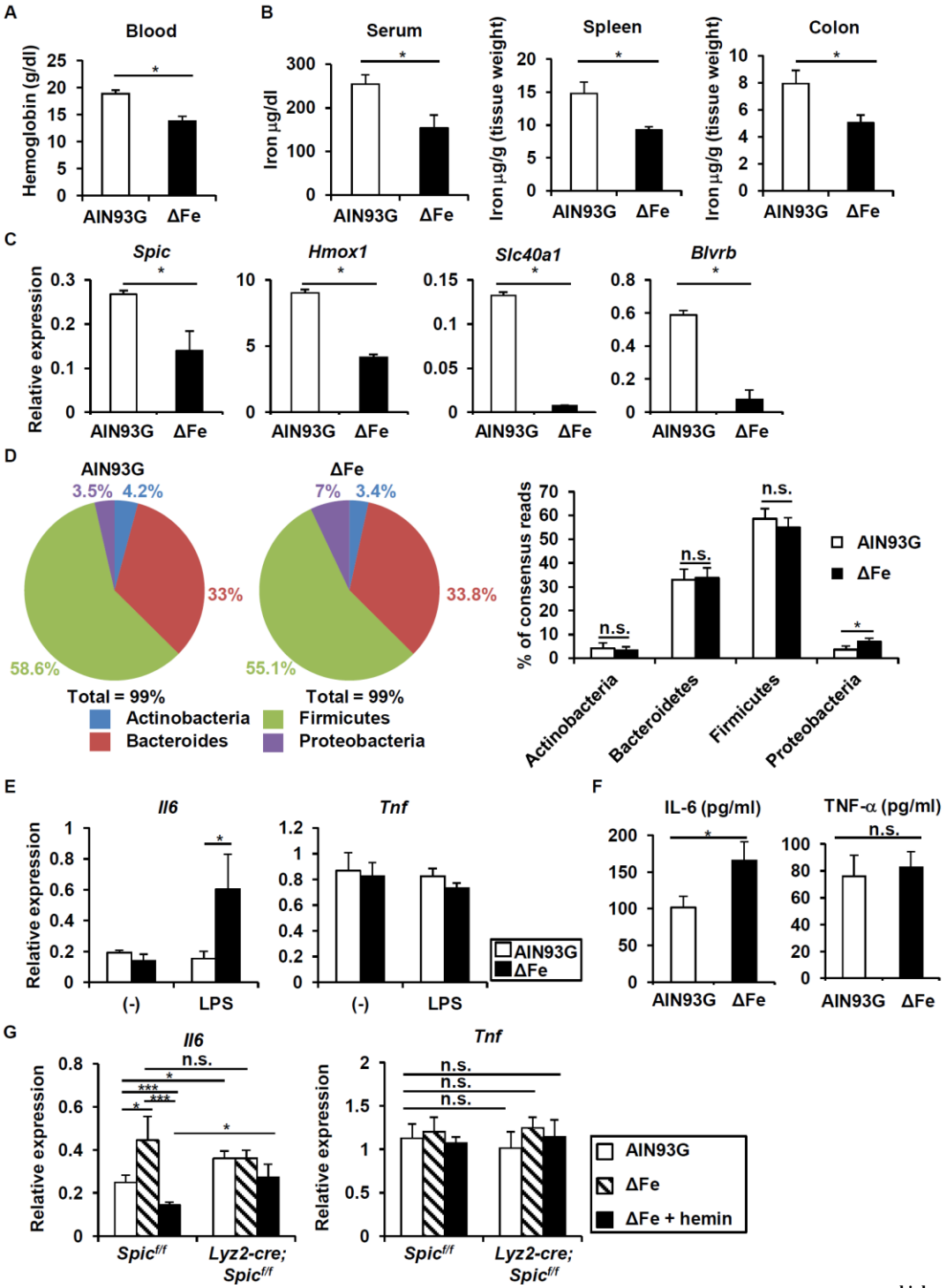

Fig. S6: Dietary iron suppresses LPS-induced *Il6* expression in large intestinal CX_3CR1^{high} Mϕs via Spi-C induction. Four or five-week-old C57BL/6J mice were fed an AIN93G or iron-reduced (ΔFe) diet for 6 or 7 weeks. **(A, B)** Concentration of hemoglobin in the blood (A) and iron in the serum, spleens, and colons (B) from mice fed the AIN93G (n = 6) or ΔFe diet (n = 9) (mean ± SEM). $^{*}p < 0.05$. All data are generated from three independent experiments. **(C)** Expression of the indicated genes in colonic CX_3CR1^{high} Mϕs from mice fed the AIN93G or ΔFe diet. Mean values ± SEM from

two separate experiments are shown (n = 4-5 per group). $^{*}p < 0.05$. **(D)** The mean abundance of the listed commensal phyla, which were determined by DNA sequencing of *16S* ribosomal DNA, in feces of C57BL/6J mice fed the AIN93G (n = 10) and ΔFe diet (n = 12) for 6 weeks (mean values ± SD). $^{*}p < 0.05$. n.s., not significant. **(E)** Expression of *Il6* and *Tnf* in colonic CX_3CR1^{high} Mϕs stimulated with or without LPS for 3 h. Mean values ± SEM are shown (n = 5 per group). $^{*}p < 0.05$. **(F)** LPS-induced production of IL-6 and TNF-α by colonic CX_3CR1^{high} Mϕs from mice fed the AIN93G or ΔFe diet (n = 14 per group). All graphs show the mean ± SEM from three independent experiments. n.s., not significant. $^{*}p < 0.05$. **(G)** Expression of *Il6* and *Tnf* in response to LPS in CX_3CR1^{high} Mϕs from mice fed with the AIN93G (n = 6) and ΔFe diet (n = 6) for 6 weeks. Hemin were injected into ΔFe diet-fed mice every other day during the last 2 weeks (n = 6). $^{*}p < 0.05$, $^{***}p < 0.005$. n.s., not significant. Graphs show the mean ± SEM. All data are of two independent experiments.

Figure S7

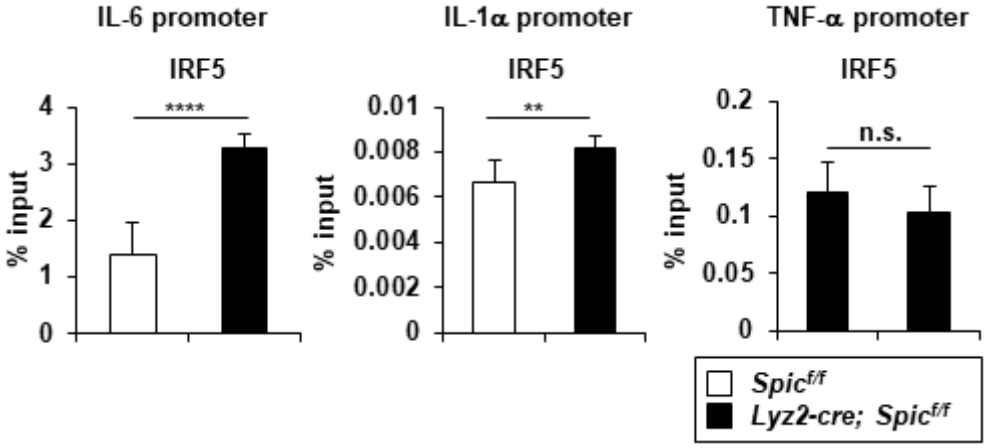

Fig. S7: Lack of Spi-C leads to increased recruitment of IRF5 to the promoter of *Il1a* and *Il6* in intestinal CX_3CR1^{high} Mϕs. ChIP assay for the *Il6*, *Il1a*, and *Tnf* promoters of NF-κB-binding site in CX_3CR1^{high} Mϕs from control and *Spic* mutant mice administered with 1.5% DSS for 7 days was performed using anti-IRF5 antibody (the mean ± SD). Data are representative of two independent experiments. $^{**}p < 0.01$, $^{****}p < 0.001$. n.s, not significant.

Table S1: Gene expression profiles in large intestinal CX3CR1^{high} Mϕs.

Probe Set ID	Representative Public ID	Gene Symbol
1436213_a_at	AV023018	1110028C15Rik
1418871_a_at	NM_025308	1810007E14Rik
1451441_at	BC026828	2210415F13Rik
1417779_at	NM_025636	2310079N02Rik
1420113_s_at	AA409325	2410022L05Rik
1435639_at	BF580962	2610528A11Rik
1416607_at	AI461712	4931406C07Rik
1452716_at	AK017688	5730469M10Rik
1429723_at	AK018153	6330409N04Rik
1418100_at	AK002962	A030009H04Rik
1419572_a_at	NM_008992	Abcd4
1422906_at	NM_011920	Abcg2
1453367_a_at	BB178770	Abhd12
1417669_at	NM_024465	Abhd12
1448894_at	NM_008012	Akr1b8
1450455_s_at	AF177041	Akr1c12 /// Akr1c13
1434987_at	AI462635	Aldh2
1460167_at	BC012407	Aldh7a1
1419114_at	AA198774	Alg14
1422573_at	D85596	Ampd3
1460330_at	AW702161	Anxa3
1426743_at	BC002232	Appl2
1452304_a_at	BC025127	Arhgef5
1416735_at	NM_019734	Asah1
1439036_a_at	AV152334	Atp1b1
1423890_x_at	BC027319	Atp1b1
1450634_at	NM_007508	Atp6v1a
1416952_at	NM_023721	Atp6v1d
1449711_at	C85064	Atp6v1e1
1418736_at	BC003835	B3galnt1
1425108_a_at	BC004728	BC004728
1415936_at	NM_013867	Bcar3
1451386_at	BC027279	Blvrb
1417381_at	NM_007572	C1qa
1449401_at	NM_007574	C1qc
1419482_at	NM_009779	C3ar1
1419483_at	NM_009779	C3ar1
1424713_at	AY061807	Calml4
1416193_at	BC011223	Car1
1448949_at	NM_007607	Car4
1460196_at	NM_007620	Cbr1
1420380_at	AF065933	Ccl2
1419561_at	NM_011337	Ccl3
1421578_at	AF128218	Ccl4
1421228_at	AF128193	Ccl7
1419684_at	NM_021443	Ccl8
1427736_a_at	AJ318863	Ccrl2
1419768_at	AF102134	Cd22
1450884_at	BB534670	Cd36
1450136_at	NM_007646	Cd38
1433741_at	BB256012	Cd38
1450494_x_at	NM_011926	Ceacam1

1423693_at	BC011218	cela1
1423153_x_at	AI987976	Cfh /// LOC100048018
1450876_at	AI987976	Cfh /// LOC100048018
1424529_s_at	BC023116	Cgref1
1436990_s_at	AA038464	Chchd10
1449402_at	AB046929	Chst7
1432418_a_at	AK018487	Ckmt1
1417089_a_at	NM_009897	Ckmt1
1448161_a_at	NM_011334	Clcn4-2
1415986_at	NM_011334	Clcn4-2
1460569_x_at	AW611462	Cldn3
1424673_at	AF350410	Clec2h
1425951_a_at	AF240358	Clec4n
1419627_s_at	NM_020001	Clec4n
1449183_at	NM_007744	Comt1
1418709_at	AF037370	Cox7a1
1448734_at	BB332449	Cp
1417496_at	BB332449	Cp
1417495_x_at	BB332449	Cp
1420617_at	NM_026252	Cpeb4
1416795_at	NM_030004	Cryl1
1448732_at	M14222	Ctsb
1417492_at	M14222	Ctsb
1451310_a_at	J02583	Ctsl
1450020_at	BC012653	Cx3cr1
1419582_at	NM_028089	Cyp2c55
1423805_at	BC006588	Dab2
1420498_a_at	NM_023118	Dab2
1430604_a_at	AW986632	Dab2
1452070_at	AK010701	Dedd2
1418287_a_at	NM_007769	Dmbt1
1418591_at	NM_021422	Dnaja4
1435680_a_at	BG067113	Dpp7
1439476_at	BG092030	Dsg2
1435493_at	AV297961	Dsp
1426314_at	BB770914	Ednrb
1423594_a_at	BB451714	Ednrb
1426607_at	BG068672	EG633640
1451161_a_at	U66888	Emr1
1419062_at	NM_013813	Epb4.1l3
1448798_at	NM_133867	Eps8l3
1450684_at	NM_007960	Etv1
1423680_at	BC026831	Fads1
1417953_at	AK016470	Fam3c
1455332_x_at	BM224327	Fcgr2b
1451941_a_at	M14216	Fcgr2b
1435476_a_at	BM224327	Fcgr2b
1425225_at	BC027310	Fcgr4
1416978_at	NM_010189	Fcgrt
1448891_at	BC016551	Fcrls
1419378_a_at	NM_052823	Fxyd2
1418207_at	NM_033648	Fxyd4
1452907_at	AK010101	Galc
1417399_at	NM_019521	Gas6
1418444_a_at	BC003902	Gde1
1418949_at	NM_011819	Gdf15

1424077_at	AK016023	Gdpd1
1417178_at	NM_016867	Gipc2
1426235_a_at	AI391218	Glul
1448303_at	NM_053110	Gpnmb
1422542_at	NM_011823	Gpr34
1455007_s_at	BI648645	Gpt2
1438385_s_at	BB068040	Gpt2
1416905_at	NM_008190	Guca2a
1418350_at	L07264	Hbegf
1450868_at	BF468249	Hgsnat
1416481_s_at	NM_019814	Higd1a
1424755_at	BB320674	Hip1
1448239_at	NM_010442	Hmox1
1419905_s_at	AV026552	Hpgd
1419821_s_at	AI788952	Idh1
1418293_at	NM_008332	Ifit2
1422305_at	NM_010510	Ifnb1
1437401_at	BG075165	Igf1
1419519_at	NM_010512	Igf1
1450330_at	NM_010548	Il10
1423017_a_at	NM_031167	Il1rn
1415911_at	NM_008378	Impact
1450029_s_at	NM_133721	Itga9
1423994_at	BQ175246	Kif1b
1451200_at	BQ175246	Kif1b
1415855_at	BB815530	Kitl
1415837_at	BC010754	Klk1
1448107_x_at	BC010754	Klk1
1426284_at	AF473907	Krt20
1423691_x_at	M21836	Krt8
1435989_x_at	AW322280	Krt8
1420647_a_at	NM_031170	Krt8
1425141_at	BE691552	Lactb2
1451336_at	BC021632	Lgals4
1424594_at	BC011507	Lgals7
1455056_at	BM231903	Lmo7
1428394_at	AK005293	Lrrc8a /// Phyhd1
1419692_a_at	NM_008521	Ltc4s
1429379_at	AV124537	Lyve1
1428667_at	AW986246	Maoa
1426244_at	BC027056	Mapre2
1431705_a_at	AK014467	Mcoln2
1422869_at	NM_008587	Mertk
1452592_at	AV066880	Mgst2
1450430_at	NM_008625	Mrc1
1419598_at	NM_026835	Ms4a6d
1424754_at	BC024402	Ms4a7
1452288_at	BG071933	Mtmr10
1424826_s_at	BC024131	Mtss1
1419754_at	NM_010864	Myo5a
1423516_a_at	BB781435	Nid2
1423086_at	BB769209	Npc1
1424265_at	BC022734	Npl
1448943_at	AK011144	Nrp1
1424339_at	AB067533	Oasl1
1431724_a_at	AK013804	P2ry12

1424453_at	BC018313	Pcyt1a
1418711_at	BB371842	Pdgfa
1449187_at	BB371842	Pdgfa
1450413_at	BC023427	Pdgfb
1449351_s_at	NM_019971	Pdgfc
1448995_at	NM_019932	Pf4
1422139_at	NM_008873	Plau
1417133_at	NM_008885	Pmp22
1418480_at	NM_023785	Ppbp
1420611_at	AV024339	Prkacb
1421492_at	NM_019455	Ptgds2
1436448_a_at	AA833146	Ptgs1
1425863_a_at	AF295638	Ptpro
1427405_s_at	BF682225	Rab11fip5
1421430_at	NM_009014	Rad51l1
1427412_s_at	BQ177183	Rapgef6
1416390_at	NM_134083	Rcbtb2
1416389_a_at	NM_134083	Rcbtb2
1449124_at	NM_016846	Rgl1
1434628_a_at	BF228009	Rhpn2
1431805_a_at	AK004849	Rhpn2
1451074_at	AF037205	Rnf13
1415749_a_at	NM_017475	Rragc
1421008_at	BB741897	Rsad2
1450788_at	NM_009117	Saa1
1419075_s_at	NM_011314	Saa1
1448005_at	BI658899	Sash1
1456080_a_at	BM239368	Serinc3
1448847_at	NM_012032	Serinc3
1450138_a_at	NM_009254	Serpinb6a
1422894_at	AV214764	Sfmbt1
1415893_at	NM_009163	Sgpl1
1417584_at	BF019859	Slc11a2
1418257_at	BB732135	Slc12a7
1428114_at	AW556396	Slc14a1
1452492_a_at	BC022752	Slc37a2
1417061_at	AF226613	Slc40a1
1417116_at	BG069516	Slc6a8
1449134_s_at	NM_011461	Spic
1450618_a_at	NM_011468	Sprr2a
1439016_x_at	AV371678	Sprr2a
1425351_at	BC011325	Srxn1
1449078_at	NM_018784	St3gal6
1450199_a_at	NM_138672	Stab1
1427072_at	BM119481	Stard8
1434803_a_at	AV050299	Sycn
1460287_at	M93954	Timp2
1452161_at	BB707122	Tiparp
1425025_at	BC022145	Tmem106a
1424354_at	BC020080	Tmem140
1448552_s_at	NM_025864	Tmem206
1424357_at	BC026654	Tmem45b
1424782_at	BC024458	Tmem77
1434768_at	AI266910	Tpp1
1448313_at	NM_009906	Tpp1
1425546_a_at	AF440692	Trf

1424649_a_at	BC025461	Tspan8
1434500_at	BF585303	Ttyh2
1416689_at	NM_011656	Tuft1
1436890_at	BG963358	Uap1l1
1417847_at	NM_013881	Ulk2
1415989_at	BB250384	Vcam1
1448162_at	BB250384	Vcam1
1451803_a_at	U48800	Vegfb
1452299_at	BI102531	Wwp1
1427098_at	BI102531	Wwp1
1424602_s_at	BC025538	Xrcc4
1438975_x_at	AV361868	Zdhhc14
1423668_at	BC021423	Zdhhc14
1437614_x_at	AV223474	Zdhhc14
1438619_x_at	BB318221	Zdhhc14
1451518_at	BC021921	Zfp709

Table S2: Spi-C-dependent LPS-inducible genes in BMDMϕs pretreated with hemin.

Symbol	Description
1190003J15Rik	RIKEN cDNA 1190003J15 gene
2200002D01Rik	RIKEN cDNA 2200002D01 gene
4833427G06Rik	RIKEN cDNA 4833427G06 gene
6530402F18Rik	RIKEN cDNA 6530402F18 gene
9130014G24Rik	RIKEN cDNA 9130014G24 gene
A130049A11Rik	RIKEN cDNA A130049A11 gene
A630012P03Rik	RIKEN cDNA A630012P03 gene
AA467197	expressed sequence AA467197
Acpp	acid phosphatase, prostate
Adhfe1	alcohol dehydrogenase, iron containing, 1
Apol9a	apolipoprotein L 9a
Apol9b	apolipoprotein L 9b
AV051173	expressed sequence AV051173
BC147527	cDNA sequence BC147527
Bend6	BEN domain containing 6
Fndc9	fibronectin type III domain containing 9
Car15	carbonic anhydrase 15
Cd38	CD38 antigen
Ch25h	cholesterol 25-hydroxylase
Cish	cytokine inducible SH2-containing protein
Cited2	Cbp/p300-interacting transactivator, with Glu/Asp-rich carboxy-terminal domain, 2
Clec4a4	C-type lectin domain family 4, member a4
Clic5	chloride intracellular channel 5
Cmpk2	cytidine monophosphate (UMP-CMP) kinase 2, mitochondrial
Cxcl11	chemokine (C-X-C motif) ligand 11
Dpep3	dipeptidase 3
Dusp14	dual specificity phosphatase 14
F3	coagulation factor III
Fam132b	family with sequence similarity 132, member B
Fam189a2	family with sequence similarity 189, member A2
Fam3b	family with sequence similarity 3, member B
Galnt3	UDP-N-acetyl-alpha-D-galactosamine:polypeptide N-acetylgalactosaminyltransferase 3
Gbp4	guanylate binding protein 4
Gdf15	growth differentiation factor 15
Gm10865	predicted gene 10865
Gm12185	predicted gene 12185
Gm14446	predicted gene 14446
Gm3086	RuvB-like protein 1 pseudogene
Gm4759	GTPase, very large interferon inducible 1 pseudogene
Gm4902	predicted gene 4902
Gm527	predicted gene 527
Gm5431	predicted gene 5431
H2-M2	histocompatibility 2, M region locus 2
Hap1	huntingtin-associated protein 1
Hilpda	hypoxia inducible lipid droplet associated

Ifit2	interferon-induced protein with tetratricopeptide repeats 2
Ifnb1	interferon beta 1, fibroblast
Igsf9	immunoglobulin superfamily, member 9
Il1a	interleukin 1 alpha
Il6	interleukin 6
Inhba	inhibin beta-A
Isg20	interferon-stimulated protein
Lpcat2	lysophosphatidylcholine acyltransferase 2
Ltf	lactotransferrin
Mmp25	matrix metallopeptidase 25
Ms4a4b	membrane-spanning 4-domains, subfamily A, member 4B
Ms4a4c	membrane-spanning 4-domains, subfamily A, member 4C
Mycl1	v-myc myelocytomatosis viral oncogene homolog 1, lung carcinoma derived (avian)
Niacr1	niacin receptor 1
Nlrc5	NLR family, CARD domain containing 5
Ntng2	netrin G2
Ocstamp	osteoclast stimulatory transmembrane protein
Olfr110	olfactory receptor 110
Olfr56	olfactory receptor 56
Osm	oncostatin M
Pcgf5	polycomb group ring finger 5
Pgf	placental growth factor
Phf11	PHD finger protein 11
Pnp2	purine-nucleoside phosphorylase 2
Rab38	RAB38, member of RAS oncogene family
Rhof	ras homolog gene family, member f
Rsad2	radical S-adenosyl methionine domain containing 2
Schip1	schwannomin interacting protein 1
Siglece	sialic acid binding Ig-like lectin E
Slfn1	schlafen 1
Slfn4	schlafen 4
Slfn9	schlafen 9
Sncg	synuclein, gamma
Tlr1	toll-like receptor 1
Tnfsf10	tumor necrosis factor (ligand) superfamily, member 10
Tpbg	trophoblast glycoprotein
Trem1	triggering receptor expressed on myeloid cells 1
Txlnb	taxilin beta
Upp1	uridine phosphorylase 1
Zbtb32	zinc finger and BTB domain containing 32

References

1. Kanki H, Suzuki H, & Itohara S (2006) High-efficiency CAG-FLPe deleter mice in C57BL/6J background. *Experimental animals* 55(2):137-141.
2. Atarashi K, *et al.* (2008) ATP drives lamina propria T(H)17 cell differentiation. *Nature* 455(7214):808-812.
3. Van der Sluis M, *et al.* (2006) Muc2-deficient mice spontaneously develop colitis, indicating that MUC2 is critical for colonic protection. *Gastroenterology* 131(1):117-129.
4. Sato A, *et al.* (2015) The Wnt5a-Ror2 axis promotes the signaling circuit between interleukin-12 and interferon-gamma in colitis. *Scientific reports* 5:10536.
5. Okumura R, *et al.* (2016) Lypd8 promotes the segregation of flagellated microbiota and colonic epithelia. *Nature* 532(7597):117-121.